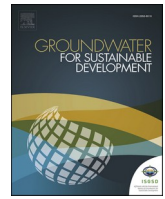




ELSEVIER

Contents lists available at ScienceDirect

## Groundwater for Sustainable Development

journal homepage: <http://www.elsevier.com/locate/gsd>

Research paper

# Integration of aeromagnetic and electrical resistivity imaging for groundwater potential assessments of coastal plain sands area of Ado-Odo/Ota in southwest Nigeria

E.S. Joel<sup>a,\*</sup>, P.I. Olasehinde<sup>b</sup>, T.A. Adagunodo<sup>a</sup>, M. Omeje<sup>a</sup>, M.L. Akinyemi<sup>a</sup>, J.S. Ojo<sup>c</sup><sup>a</sup> Department of Physics, Covenant University Ota, Nigeria<sup>b</sup> Department of Geophysics, University of Ilorin Kwara State, Nigeria<sup>c</sup> Department of Applied Geophysics, Federal University of Technology Akure, Ondo State, Nigeria

## ARTICLE INFO

## Keywords:

Groundwater potential  
Aeromagnetic technique  
Sedimentary rock  
Borehole drillers  
Electrical resistivity imaging  
Nigeria

## ABSTRACT

This study aims to investigate the groundwater potential of Coastal Plain Sands area of Ado-Odo/Ota within Dahomey Basin using the integration of aeromagnetic method and electrical resistivity imaging. The aeromagnetic method is applied to reveal the possible hydrogeological structures (such as lineament or fracture) buried in the subsurface. The lineaments which are interconnected are observed in the eastern part of the study area while the western part is void of the interconnectivity of lineaments. Resistivity technique is applied in regions where there are interconnectivity and non-interconnectivity of lineament to delineate occurrence of groundwater about the observed lineament. The depths to magnetic sources range between 102.6 and 1965.2 m. Furthermore, the result of resistivity technique shows that the depth to aquifer ranges from 40 to 100 m with corresponding resistivity values that range between 150.0 and 350.0  $\Omega\text{m}$  in the region of the interconnectivity of lineament, which is the eastern part of the study area (Igboloye-Covenant University area) and had high groundwater potential. The western part which is void of the interconnectivity of lineaments (Alapoti area) ranges from 80 to 130 m with resistivity values that range between 250.0 and 450.0  $\Omega\text{m}$  suggesting that the area has low groundwater potential. The study, therefore, shows that the occurrence of groundwater in Ado-Odo/Ota community is a function of hydrogeological structures such as lineaments or fractures, and as a result, this information could serve as guide for borehole drillers, civil engineers and resident of the study area for proper planning before siting borehole either for domestic or industrial use.

## 1. Introduction

It has been confirmed that groundwater exists in the three main rocks types that are found in the earth crust namely the igneous, sedimentary and metamorphic rocks, and each of these rocks that host the groundwater needs to be carefully studied to derive maximum benefit (Vouillamoz et al., 2015). Exploration of groundwater is usually a hydrogeological and hydro-geophysical inference operation and depends on the analysis of the hydrological indicators and assurance (Anthony, 2012). As a result, groundwater has been adjudged to offer an abundance of water to a man (Olasehinde, 2010; Omole, 2013; Omole and Ndambuki, 2014; Adagunodo et al., 2018a) which is a reliable and most constant source of water supply in terms of quantity and quality. Due to its invisibility on the earth subsurface and probable

misinformation about its existence, many have not placed value on groundwater as the only source of sustainable water supply. However, the occurrence of groundwater in any part of the surface of the earth is not a matter of chance but as a result of the interaction of physio-graphical, ecological, hydrological, geological, and climatic factors (Biswas et al., 2012; McLachlan et al., 2017). Therefore, exploring groundwater resource requires the use of certain geophysical techniques to derive its benefits. Various geophysical methods have been employed in exploring groundwater resources ranging from traditional methods (such as fracture trace method) to sophisticated ones (which include electrical, electromagnetic, seismic methods, etc.). However, recently, it has been observed that using any geophysical techniques alone for groundwater investigation might not yield desired result (Omole, 2013; Descloitres et al., 2013; Ojo et al., 2015) and this is due to the

\* Corresponding author.

E-mail address: [emmanuel.joel@covenantuniversity.edu.ng](mailto:emmanuel.joel@covenantuniversity.edu.ng) (E.S. Joel).<https://doi.org/10.1016/j.gsd.2019.100264>

Received 1 August 2018; Received in revised form 16 August 2019; Accepted 19 August 2019

Available online 22 August 2019

2352-801X/© 2019 Elsevier B.V. All rights reserved.



## 2. Materials and methods

### 2.1. Study area

The Ado-Odo/Ota area (Fig. 1) is within the Dahomey basin which is one of the sedimentary terrains of Nigeria and located at the southern part of Ogun State sharing boundary with Lagos State and is characterised by lowlands, valleys and hills (undulating terrain). The pattern of drainage of the study area is dendritic. The area drained by Iju River, River Imede, River Isaku, River Ogbe, River Owuru, River Ore, River Imojiba and other tributaries. It has an area of 878 km<sup>2</sup> and a population of about 526,565 at the 2006 census. The distance between the study area and Lagos lagoon is about 121 km while the mean elevation is about 200 m above the sea level. Generally, Arabian and African continent is made up of a Precambrian basement of crystalline meta-sedimentary, igneous and meta-igneous rocks (Adagunodo et al., 2018b). This crystalline basement is overlain by a series of geological settings ranging from volcanic and sedimentary sequences to unconsolidated Cenozoic sediments (Adagunodo et al., 2018c; Adewoyin et al., 2017). Nigeria is on the Pan-African mobile belt, which separates the Congo Cratons and the West African Craton. The two major geological formations that spread in equal proportion in Nigeria are the sedimentary Basins (Upper Cretaceous in age) and Basement rocks (Precambrian in age) (Adagunodo et al., 2018c; Adewoyin et al., 2017). The local geology of the study area is made up of sedimentary rock sequence of Dahomey Basin (Fig. 2)

which extends from the eastern part of Ghana through Togo and Benin Republic to the western margin of the Niger Delta. The geological succession in the basin is as follows: the structure of the basin is a simple monocline against the basement which underlies the sedimentary rocks at varying depths. The dips are reportedly 1° or less to the south and southwest (Jones and Hockey, 1964). The sequence of the rocks underlying the study area is as follows: Abeokuta Formation which is Cretaceous in age (Senonia) and this formation lies conformably on the Basement Complex in the north and Ewekoro Formation in the north-east. It is the oldest sedimentary formation, having a thickness of 250–300 m (Reyment, 1965; Offodile, 2002). It consists of arkosic sandstones and grits, tending to be carbonaceous towards the base (Offodile, 2002). Overlying the Abeokuta Formation is Ewekoro/Oshosun/Akinbo Formation, which is Paleocene. The formation consists of a series of sandstone, shales, limestones and clays varying between 100 and 300 m in thickness. This formation overlaid by Ilaro Formation (Tertiary age - Eocene). It consists of fine to coarse sands alternating with shales and clays (Offodile, 2002). Ilaro Formation is overlaid by coastal plain sands (Pliocene) and Recent Alluvium (Quaternary age) of Benin Formation, which is the youngest. The formation comprises of sandstones and shales of upper Ilaro Formation, the sequence of predominant continental sands and some lenses of shales and clays which is about 107.7 m thick (Reyment, 1965; Offodile, 2002).

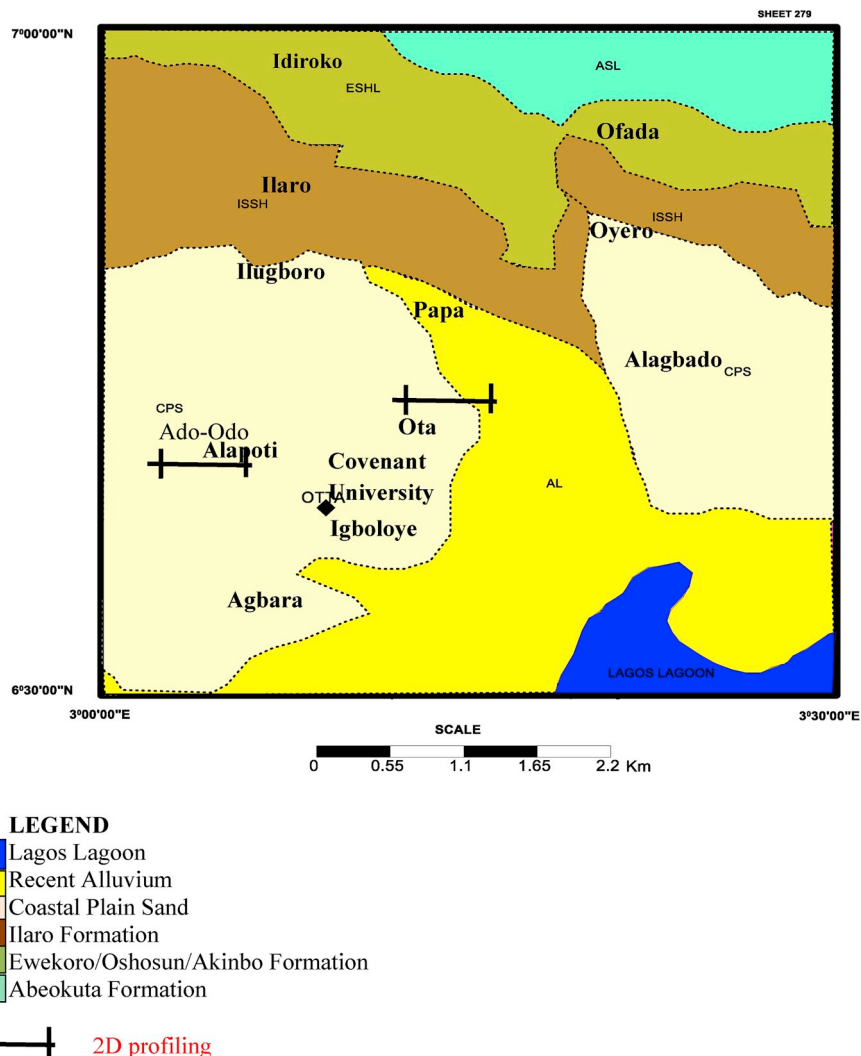


Fig. 2. Local geological map of the study area showing 2D profiling section.

## 2.2. Aeromagnetic method

The aeromagnetic method involves the use of aircraft to conduct a magnetic survey to investigate the subsurface. This technique makes use of variation in the earth magnetic field as the detecting tool (Adagunodo et al., 2017). Magnetic field variations often used as diagnostics of minerals and regional structures. In magnetic prospecting, the main target of the application is the primary field which varies slowly and is of internal origin, small field – this varies rapidly and originates outside the earth and spatial variations of the main field which are smaller compared to main field (Telford et al., 1990). These parameters are usually constant with time and place and is caused by local magnetic anomalies in the near-surface of the crust of the earth (Telford et al., 1990).

### 2.2.1. Description of an analytical signal

Analytical Signal (AS) is known as total gradient and defined as the square root of the sum of vertical derivatives of total magnetic field intensity in the x, y and z directions. Analytical Signal requires the horizontal (x, y) derivatives of the total magnetic field of the first-order vertical derivative (z). Roest et al. (1992) and MacLeod et al. (1993) described that analytical signal could be computed in 3D format from three orthogonal derivatives of the total magnetic field intensity using the expression:

$$|ASIG(x,y)| = \left[ \frac{\partial F}{\partial x} \left( (x,y)^2 \right) + \left( \frac{\partial F}{\partial y} \left( x,y \right) \right)^2 + \left( \frac{\partial F}{\partial z} \left( x,y \right) \right)^2 \right]^{\frac{1}{2}} \quad (1)$$

where ASIG is analytical signal and F is observed total magnetic field at (x, y). Space domain analysis using splines are used in horizontal derivatives computation, and wavenumber domain using fast Fourier transform are used for vertical gradient computation (Al-Garni, 2010).

### 2.2.2. Tilt derivative analysis

Tilt derivative also is known as tilt angle derivative (Miller and Singh, 1994; Verduzco et al., 2004) is defined as

$$\theta = \left[ \begin{array}{c} \frac{\partial F}{\partial z} \\ \frac{\partial F}{\partial h} \end{array} \right] \quad (2)$$

where

$$\frac{\partial F}{\partial h} = \sqrt{\left( \frac{\partial F}{\partial x} \right)^2 + \left( \frac{\partial F}{\partial y} \right)^2} \quad (3)$$

and  $\partial F/\partial x$ ,  $\partial F/\partial y$  and  $\partial F/\partial z$  are the derivatives of the magnetic field  $\vec{H}$  in the x, y and z-direction. Salem et al. (2007) defined the rate of change of the tilt angle derivative  $\Theta$  concerning the x, y, and z directions as the wave-numbers

$$K_x = \frac{\partial \theta}{\partial x} = \frac{1}{A^2} \left( \frac{\partial F}{\partial h} \frac{\partial^2 F}{\partial x \partial h} - \frac{\partial F}{\partial z} \left( \frac{\partial F}{\partial h} \right)^{-1} \times \left( \frac{\partial F}{\partial x} \frac{\partial^2 F}{\partial x^2} + \frac{\partial F}{\partial y} \frac{\partial^2 F}{\partial y \partial x} \right) \right) \quad (4)$$

$$K_y = \frac{\partial \theta}{\partial y} = \frac{1}{A^2} \left( \frac{\partial F}{\partial h} \frac{\partial^2 F}{\partial y \partial h} - \frac{\partial F}{\partial z} \left( \frac{\partial F}{\partial h} \right)^{-1} \times \left( \frac{\partial F}{\partial y} \frac{\partial^2 F}{\partial y^2} + \frac{\partial F}{\partial x} \frac{\partial^2 F}{\partial x \partial y} \right) \right) \quad (5)$$

$$K_z = \frac{\partial \theta}{\partial z} = \frac{1}{A^2} \left( \frac{\partial F}{\partial h} \frac{\partial^2 F}{\partial z^2} - \frac{\partial F}{\partial z} \left( \frac{\partial F}{\partial h} \right)^{-1} \times \left( \frac{\partial F}{\partial x} \frac{\partial^2 F}{\partial x \partial z} + \frac{\partial F}{\partial y} \frac{\partial^2 F}{\partial y \partial z} \right) \right) \quad (6)$$

where

$$A = \sqrt{\left( \frac{\partial F}{\partial x} \right)^2 + \left( \frac{\partial F}{\partial y} \right)^2} + \sqrt{\left( \frac{\partial F}{\partial z} \right)^2} \quad (7)$$

and is the total gradient magnetic field.

### 2.2.3. Source parameter imaging

Source Parameter Imaging (SPI) is a powerful, easy and quick method for determining magnetic sources depth (thickness of sediment). It has an accuracy of about ( $\pm$ ) 20% which is similar to that of Euler deconvolution, but source parameter imaging (SPI) has the benefits that it can produce a complete set of coherent solution points and it can easily be used. The goal of SPI is that resulting images can easily be interpreted by an expert geologist (Thurston and Smith, 1997). Thurston and Smith (1997) determined the depth from the local wave-number of the analytical signal using SPI method and defined by Nabighian (1972) as:

$$A_1(X, Z) = \frac{\partial F(x, z)}{\partial x} - j \frac{\partial F(x, z)}{\partial z} \quad (8)$$

where F(x, z) is the anomalous total magnetic field (TMF) while j is the imaginary number, z and x are Cartesian coordinates for both vertical and horizontal directions respectively.

## 2.3. Aeromagnetic data acquisition

Aeromagnetic data on sheet 279 on a scale of 1: 100,000 and on the coverage area of 3025 Sq. Km was acquired from Nigeria Geological Survey Agency (NGSA), which was collected between 2006 and 2009 and covered the study area. The Mean Terrain Clearance (MTC) used during the acquisition is 80 m. The equipment used for the acquisition of the data by the NGSA is 3 Scintrex Cesium vapour magnetometers mounted in about 7 Cessna Caravan fixed-wing aircraft, the data recording interval was 0.1 s or less than 7 m and flight line spacing of 500 m. Projection method used in processing the data was the Universal Transverse Mercator (UTM) and the WGS 84 as a datum. The spheroid model used was the Clarke 1880 (modified), 33°E central meridian, a scaling factor of 0.9996, a 500,000 m X Bias, a 0 m Y Bias and 50 m grid mesh size were the plotting specification and IGRF 2005 model was used for the calculation of declination and inclination. The first step in processing the aeromagnetic data was to digitize the data acquired and produce Total Magnetic Intensity map (TMI) that covers the study area using Oasis montaj software version 6.4 (Fig. 3). The second step involved analytical studies which were carried out using interpretation techniques. The interpretation techniques used include analytical signal, tilt derivative analysis and source parameter imaging (the procedure is described in section 2.1.1 - 2.1.3) using version 6.4 of Oasis montaj software.

## 2.4. Electrical resistivity principle

One of the new developments in recent years is the use of 2-D electrical imaging/tomography surveys to map subsurface geology (Adagunodo et al., 2015), such surveys are usually carried out using a large number of electrodes, 25 or more, connected to a multi-core cable. A laptop microcomputer together with an electronic switching unit is used to select the relevant four electrodes for each measurement automatically. At present, field techniques and equipment to carry out 2-D resistivity surveys are fairly well developed. The necessary field equipment is commercially available from several international companies (Adagunodo et al., 2015). In electrical resistivity technique, two pairs of electrodes are used for the fieldwork. The outer two electrodes are typically the current (source) electrodes, and the inner two electrodes are the potential (receiver/sink) electrodes. The array spacing expands about the array midpoint while maintaining an equivalent spacing between each electrode (Keller and Frischknecht, 1966). The resistivity measurements are usually made by injecting current into the ground through two electrodes and measuring the resulting voltage difference at two potential electrodes. From the current (I) and Voltage (V) values, an apparent resistivity ( $\rho_a$ ) value can be estimated as shown



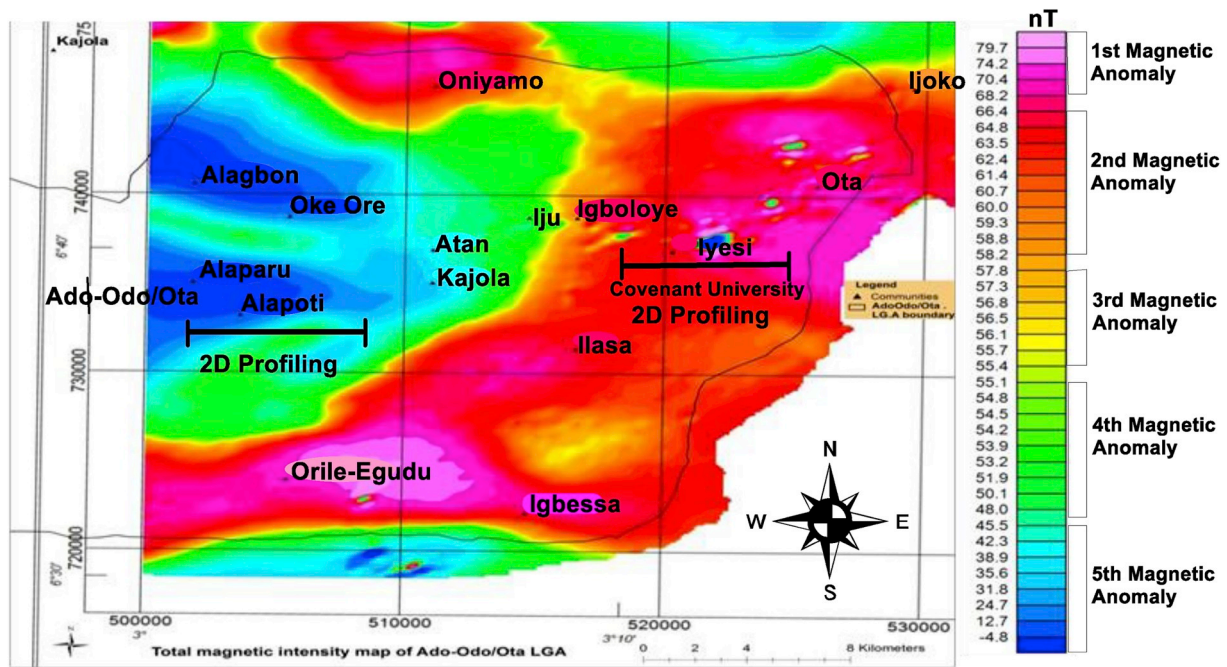


Fig. 3. Total magnetic intensity map that covers Ado-Odo/Ota showing 2D profiling section taken within geological units of Recent alluvium and Coastal Plains Sand.

in Eq. (9). Wenner array (with multi-electrodes) is usually adopted for 2-D imaging (Adagunodo et al., 2015). This array is suitable to map the lateral subsurface variations within the investigated region.

$$\rho_a = 2\pi a \frac{V}{I} \quad (9)$$

where the  $\rho_a$  is measured in  $\Omega.m$ ,  $V$  is measured in volt;  $I$  is measured in Ampere,  $a$  is the electrode spacing in meter, while  $2\pi a$  is known as the geometric factor.

The advantages of the Wenner array are that the apparent resistivity can be calculated quickly in the field and the instrument sensitivity is not as crucial as with other array geometries. Relatively small current magnitudes are needed to produce measurable potential differences (EPA, 1993). The disadvantages are that for each sounding, all of the electrodes have to be moved to a new position. Imaging deep into the earth, it is necessary to use longer current cables; handling the cables and electrodes between each measurement can be cumbersome, especially in steep terrain. The Wenner array is also very sensitive to near-surface inhomogeneity, which may skew, more in-depth electrical responses.

### 2.5. Electrical resistivity data acquisition

In this research, 2D resistivity profiling using Wenner configuration (Fig. 2) was adopted with the aid of the ABEM Terrameter SAS 1000 series in obtaining the resistivity data. The arrangement of profiling used for the acquisition of resistivity data in this work is Wenner array with the profiles length of 400 m and 1200 m respectively. The 2D resistivity data was interpreted using DIPROfWin software version 4. The absolute error (RMS) of  $\pm 0.58$  was achieved at five (5) iterations. Other materials used are four (4) hammers, two (2) current cables and two (2) potential cables which are the connecting cables between the electrodes and the terrameter, four (4) tape rules for profile length measurement, 75 electrodes, walking talking, four (4) clips and a car battery.

## 3. Result and discussions

### 3.1. Aeromagnetic responses of aeromagnetic data

Fig. 3 shows the total magnetic intensity of over Ado-Odo/Ota. The first magnetic anomaly of interest was the high magnetic value ranging between 68.2 and 80.0 nT. These are found trending in the eastern, southern and north-west part respectively. The second magnetic anomaly had high magnetic intensity value ranging between 58.2 and 66.4 nT. The third magnetic anomaly represented semi-intermediate magnetic anomalies ranging between 55.4 and 57.8 nT. The fourth anomaly had magnetic intensity values that ranged between 47.0 and 55.1 nT. The fifth magnetic anomaly has TMI values that range between - 4.8 and 45.5 nT. Geologically, the first, second, third and fourth magnetic anomalies represented shallow Basement Complex rocks judging from the high magnetic intensity value observed which is a reflection of typical igneous and metamorphic rocks while the fifth magnetic anomalies represent Sedimentary terrain. In terms of rock types; first, second and third magnetic anomalies indicated the presence of igneous rock, the fourth magnetic anomalies represent metamorphic rock, and the fifth magnetic anomalies represent sedimentary rock. The observed geological variations that existed in the area are essential in understanding the hydrogeological situation of the study area, particularly in terms of groundwater potential.

### 3.2. Analytical signal of aeromagnetic data

The advantage of this interpretation technique is that its shape is independent of the direction of magnetisation of the source body and the ambient field as well (Roest et al., 1992; MacLeod et al., 1993). As a result of this, the analytical signal is beneficial at low magnetic latitude. Ridges or peaks in analytical signal total magnetic intensity anomaly map occur mostly on geological targets such as faults, volcanic plugs, dykes, shear zones, lithological contacts, discrete bodies, and their edges, magnetisation's directions notwithstanding (Roest et al., 1992; Wijns et al., 2005; Anudu et al., 2014). The analytical signal map of Ilaro sheet 279 shows some anomalies bodies in the area (Fig. 4). Analytical signal map of the aeromagnetic data of the study area confirms that the

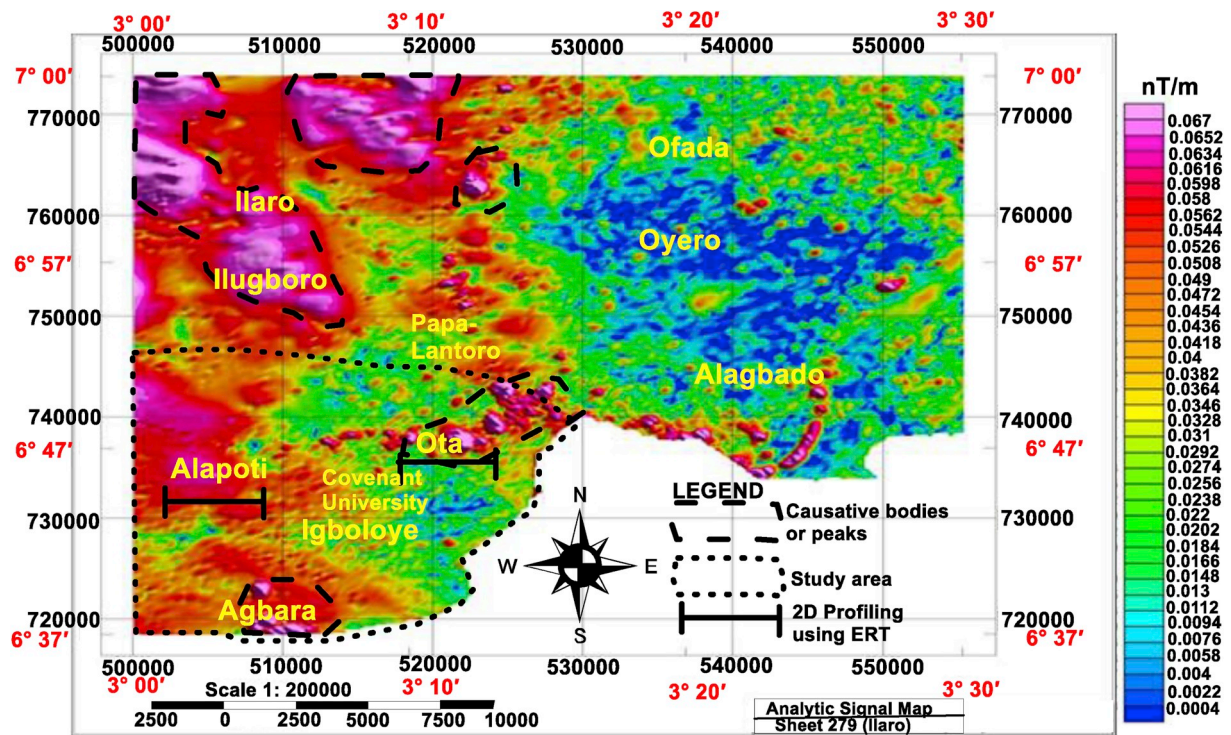


Fig. 4. Analytical signal map showing some causative bodies.

anomalies peaks exist over the causative bodies (this is shown in Fig. 4 using dash line circle as a demarcation) which can be as a result of thick sedimentary underlying the sedimentary formation in the study area. The probable causative bodies scattered within the central part of the study area towards the east and south were observed. Moreover, this depicts the structural elements that can control the groundwater occurrence in the southern and eastern part of the study area.

### 3.3. Tilt derivative of aeromagnetic data

Tilt derivative analysis map is shown in Fig. 5 and; this described the presence of lineaments in the study area and concentrated in the eastern part of the study area. The lineaments pattern is a northwest-southeast and northeast-southwest structural trend. Two geological environments (shallow Basement Complex and sedimentary terrain) were

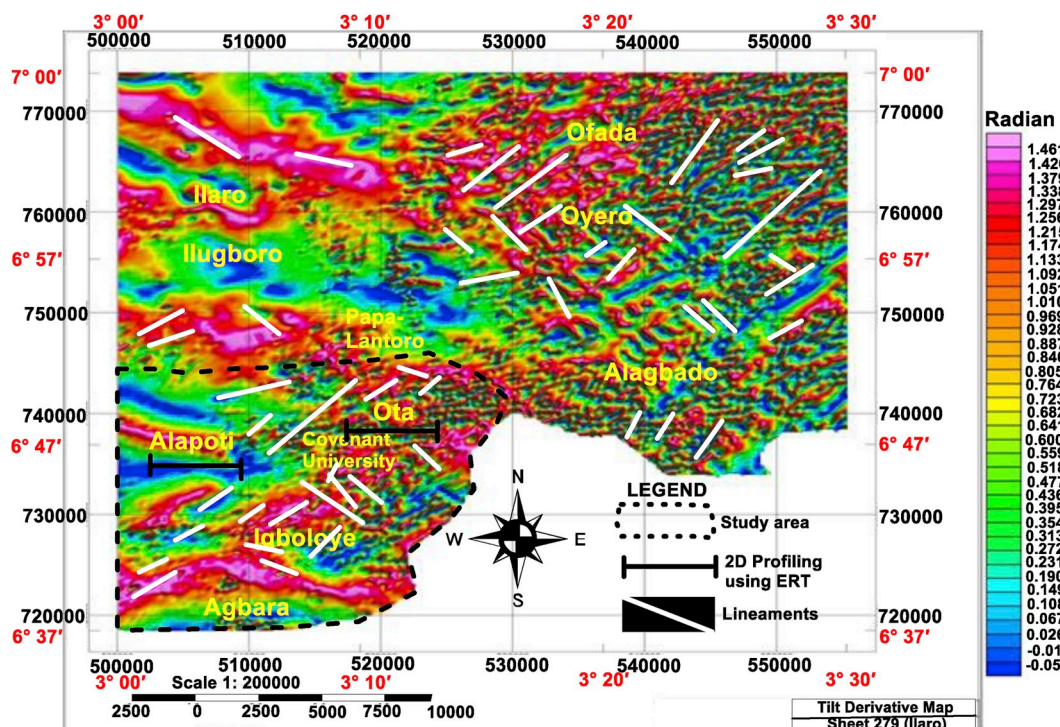


Fig. 5. Tilt derivative map for locating lineaments feature.



indicated in Fig. 5; however, shallow basement rock sources dominated the north-east and south-east region and partly the southern region. However, the sedimentary terrain was deep-seated and shallow basement sources occurring at a depth ranging between 102.6 m and 663.0 m (this was inferred using source parameter imaging as shown in Fig. 6). This indicates that in the north-east and south-east regions, there are linear structures which are probably fractures, which are pronounced in the region compared to the western part of the study area. Furthermore, it is also implied that in eastern region groundwater could be as a result of fracturing and not thick sedimentary cover. The presence of lineaments in the study area could be as a result of shallow basement rock intruded into the basin. These lineaments may likely be groundwater channels which might serve as groundwater aquifer.

### 3.4. Source parameter imaging

Source parameter imaging (SPI) is used mostly for determining the depth to magnetic sources when interpreting aeromagnetic data over an area, and this was used to determine the thickness of the basin that overlies the basement complex. The western part of the study area is shown as deep-seated sources, and the eastern area is shallow source area (Fig. 6). The western area has the depth to magnetic sources greater than 500 m; the intermediate magnetic sources have a depth ranging between 200 m and 500 m. While shallow sources on the eastern side have depths less than 200 m. The shallow sources originated from shallow basement complex rocks, and it has a thickness of about 200 m. This is pronounced in the eastern, south-eastern and partly south. However, the thickness of sedimentary rock that covers the underground basement rock of the basin ranged from 710.2 m to 1965.2 m and is pronounced in the north-western part. In the study area, the first layer,

which is Recent Alluvium varied from 824 m to 1952 m with a thickness of 1128 m (a colour indication of light blue to pure blue). It was observed that the first layer at Alapoti could be cross-bedded sand of Benin Formation, which is greenish and could underlay the topsoil. The thickness ranged between 413 m and 763 m and the minimum thickness of about 350 m. It is clearer from Fig. 6 that Alapoti area with thick overburden and substantial intercalation of sand and silt could be viable for groundwater potential. The extension towards the eastern part of Alapoti area is Igboloye where Covenant University Ota and its environs are situated on the southern part of the study area. It can be seen that the recent alluvium formed in the area is about 61 m thick with the depth that ranged from 763 m to 824 m. The Benin Formation (depicted in green colour) and Ilaro, Ewekoro/Oshosun/Akinbo Formation coupled with Abeokuta Formation and shallow basement complex (which are depicted red and pink) varied in depths from 386 m to 763 m with a thickness of about 377 m. The depth of Ilaro Formation (yellowish) at Igboloye area varied from 246 m to 362 m with a thickness of about 116 m. This Igboloye area, however, could be weathered with fissures that may serve as water-bearing conduits. The basement depth ranged from 102 m to 231 m with a mean value of 129 m thick.

### 4. Electrical resistivity of alapoti area

Electrical resistivity imaging was carried out at Alapoti and Igboloye areas (Figs. 7 and 8) where Covenant University is situated. Alapoti is on the western edge and situated where the magnetic intensity is low, while Covenant University is situated on the high magnetic intensity region, as revealed in Fig. 3. The source parameter imaging reveals that Alapoti area has a deep-seated source while the Covenant University depicts shallow magnetic source depths. Figs. 7 and 8 are composed of three

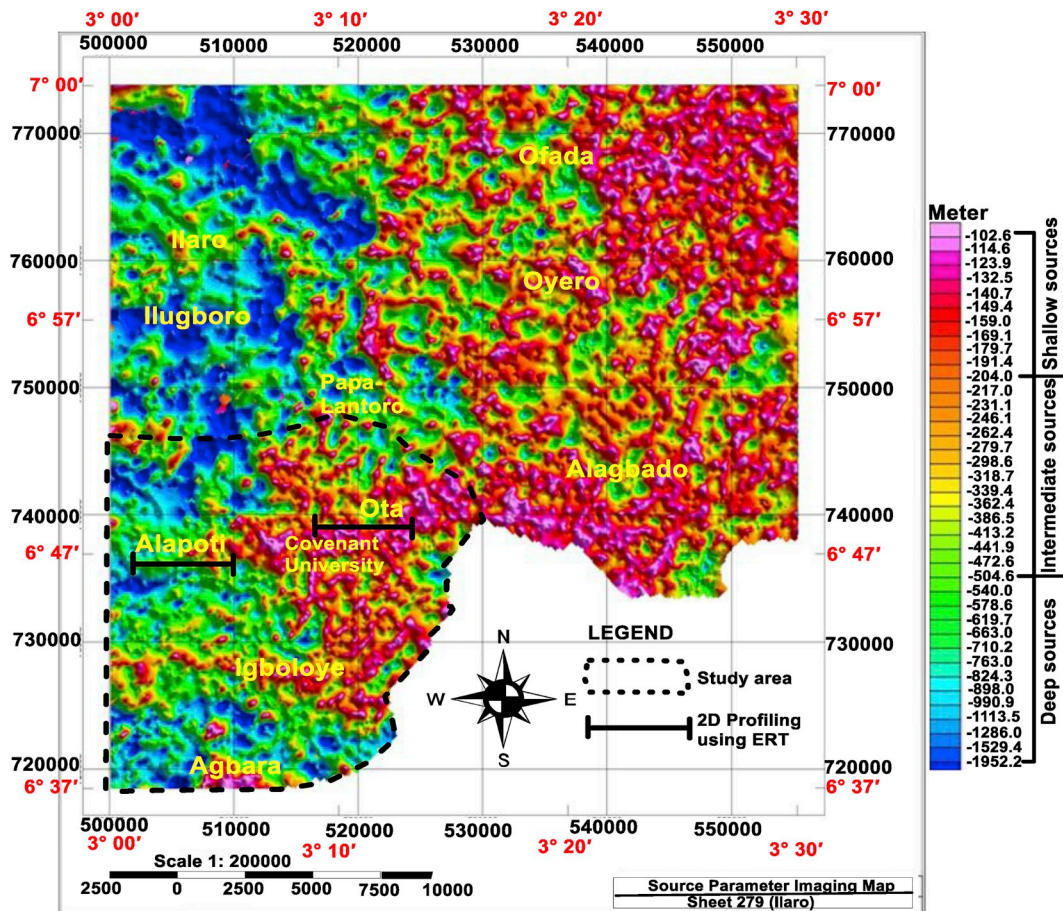


Fig. 6. Map of source parameter imaging for depth to the magnetic source.

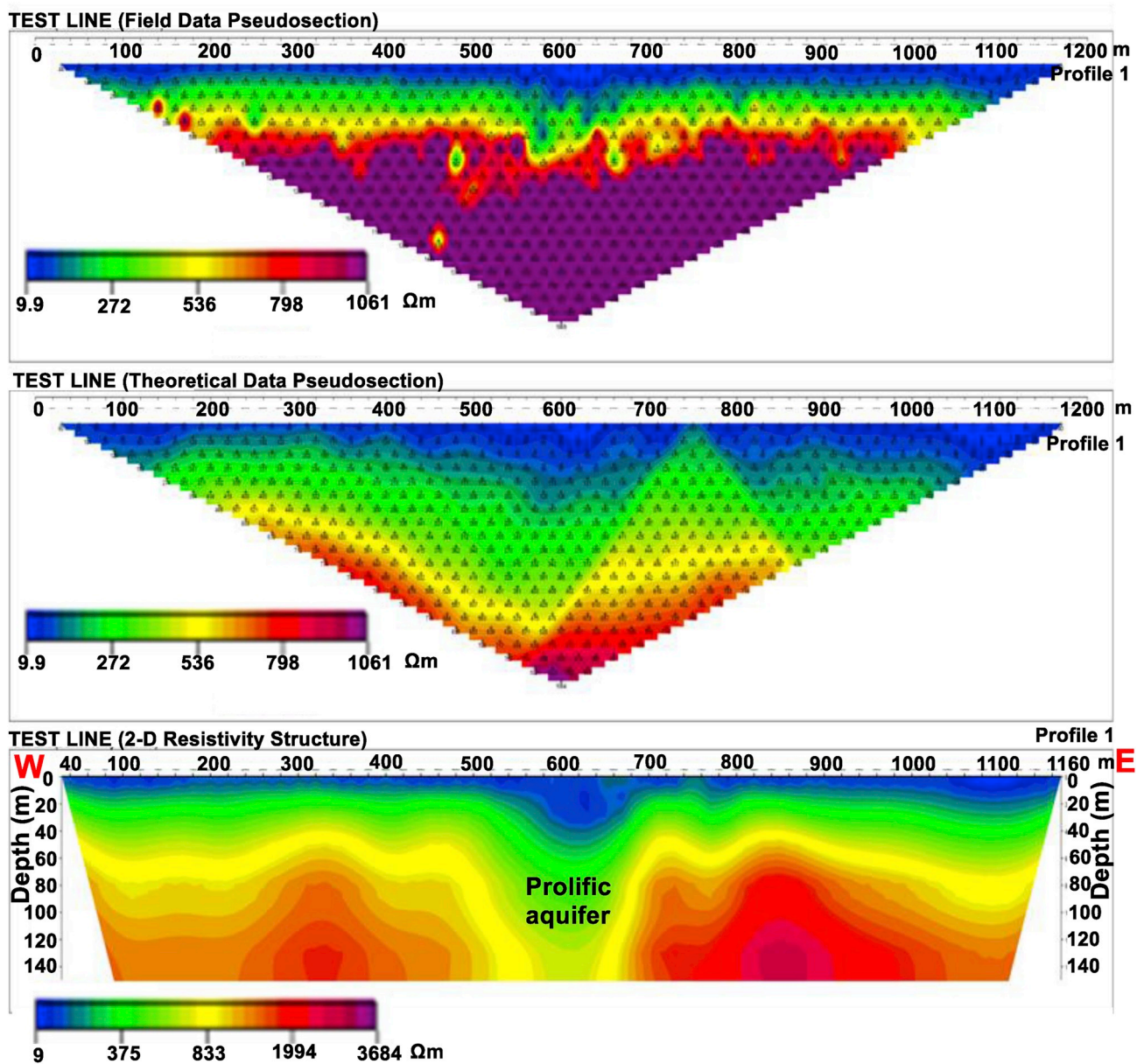


Fig. 7. 2D Resistivity Profiling section taken at Alapoti area.

images each. The first imaging is the display of the measured apparent resistivity on the field as plotted by DIPROwin software. The second imaging is the analytical data, which compares the standard model with the field data (image matching technique) (Adagunodo et al., 2015). The third imaging is the 2-D resistivity map that gives the final model of the subsurface. The 2-D resistivity map is used to assess the lithologic variations within the subsurface (Aizebeokhai et al., 2016). In the Post Precambrian settings (that is, consolidated sedimentary rocks) (Aizebeokhai et al., 2016; Oyeyemi et al., 2018) prolific groundwater could be explored within sandstones or limestones strata (Oyeyemi et al., 2018). The result of 2-dimensional resistivity profiling taking from Alapoti indicates that the aquifer (sandstones) resistivity ranged between 250.0 and 450.0  $\Omega\text{m}$  at a depth of 80–130 m (Fig. 7), while that of Igboloye area where Covenant University is situated ranged between 150.0 and 350.0  $\Omega\text{m}$  at the depth to the aquiferous unit (sandstones) which varied between 40 and 70 m. The depth to aquiferous strata delineated using 2-D resistivity profiling in Covenant University, Ota agrees with the results of (Oyeyemi et al., 2018), who reported that depth to aquiferous units varied between 34.0 and 77.0 m in Iyana-Iyesi,

Ota using vertical electrical sounding. In addition, when the depth to aquiferous zones obtained from this present study were compared with the results of Oyeyemi et al. (2018) and Joel et al. (2016) that were obtained in the proximity of this present study, it was observed that the delineated aquifer's depths in this study were in agreement with those results.

## 5. Conclusions

The potential groundwater assessments in coastal plain sands area of Ado-Odo/Ota have been made using the integration of aeromagnetic and electrical resistivity imaging. The aeromagnetic method reveals that hydrogeological structures (such as lineament or fracture) are buried in the subsurface of the study area. Resistivity technique has been applied in regions where there are interconnectivity and non-interconnectivity of lineament to delineate occurrence of groundwater concerning the observed lineament. Furthermore, the study shows there are presences of lineaments that are interconnected, which host groundwater in the southern and eastern part of the study area as observed from tilt



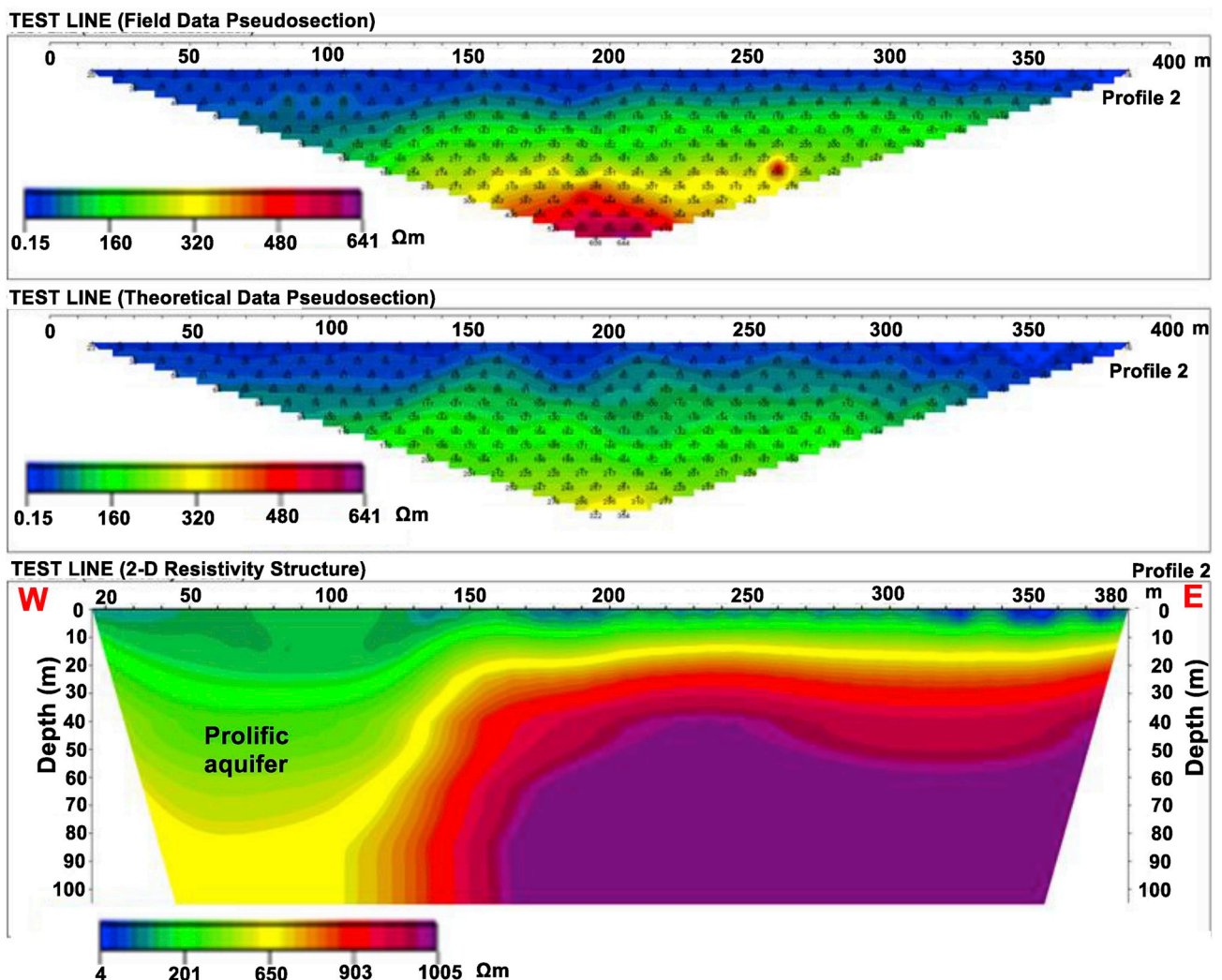


Fig. 8. 2D resistivity profiling section within Covenant University (Igboloye area).

derivative map. The area of high magnetic anomalies has the shallow depth that ranges between 102.6 and 169.1 m, while the area of low magnetic anomalies (western part of the study area) has a deeper depth of about 710.2 to approximately 2000 m. The result of resistivity technique shows that the depth to aquifer ranges from 40 to 100 m, with corresponding resistivity values that range between 150.0 and 350.0  $\Omega\text{m}$  in the eastern part of the study area (Igboloye-Covenant University area). This part of the study area had high groundwater potential, while the western part which is void of the interconnectivity of lineaments (Alapoti area) ranges from 80 to 130 m, with resistivity values that range between 250.0 and 450.0  $\Omega\text{m}$ . The study, therefore, showed that the occurrence of groundwater in the eastern part of Ado-Odo/Ota is primarily controlled by lineaments (fractures), while the existence of lineaments in western part suggests depth at which borehole should be drilled to avoid waste of money and energy in drilling abortive boreholes.

#### Acknowledgement

The researchers appreciate Covenant University Ota for financial support in carrying out this research. Also, the untiring effort of the handling editor and reviewers of this article is highly appreciated.

#### Appendix A. Supplementary data

Supplementary data to this article can be found online at <https://doi.org/10.1016/j.gsd.2019.100264>.

#### References

- Adagunodo, T.A., Akinloye, M.K., Sunmonu, L.A., Aizebeokhai, A.P., Oyeyemi, K.D., Abodunrin, F.O., 2018. Groundwater exploration in aaba residential area of akure, Nigeria. *Front. Earth Sci.* 6, 66. <https://doi.org/10.3389/feart.2018.00066>.
- Adagunodo, T.A., Lüning, S., Adeleke, A.M., Omidiora, J.O., Aizebeokhai, A.P., Oyeyemi, K.D., Hamed, O.S., 2018. Evaluation of  $0 \leq M \leq 8$  earthquake data sets in the african-asian region during 1966 – 2015. *Data in Brief* 17C, 588–603. <https://doi.org/10.1016/j.dib.2018.01.049>.
- Adagunodo, T.A., Hamed, O.S., Usikalu, M.R., Ayara, W.A., Ravisankar, R., 2018. Data on the radiometric survey over a kaolinitic terrain in Dahomey basin, Nigeria. *Data in Brief* 18C, 814–822. <https://doi.org/10.1016/j.dib.2018.03.088>.
- Adagunodo, T.A., Adeniji, A.A., Erinle, A.V., Akinwumi, S.A., Adewoyin, O.O., Joel, E.S., Kayode, O.T., 2017. Geophysical investigation into the integrity of a reclaimed open dumpsite for civil engineering purpose. *Interciencia Journal* 42 (11), 324–339.
- Adagunodo, T.A., Sunmonu, L.A., Adeniji, A.A., 2015. Effect of dynamic pattern of the saprolitic zone and its basement on building stability: a case study of a high-rise building in ogbomososo. *J. Appl. Phys. Sci. Int.* 3 (3), 106–115.
- Adewoyin, O.O., Joshua, E.O., Akinyemi, M.L., Omeje, M., Joel, E.S., 2017. Investigation to determine the vulnerability of reclaimed land to building collapse using the near-surface geophysical method. *IOP Conf. Series: J. Phys. Conf. Ser.* 852.
- Al-Garni, M.A., 2010. Magnetic survey for delineating subsurface structures and estimating magnetic sources depth, Wadi Fatimah, KSA. *J. King Saud Univ. Sci.* 22, 87–96.

- Anthony, R.A., 2012. Azimuthal square array resistivity method and groundwater exploration in Sanganoor, Coimbatore District, Tamilnadu, India. *Research Journal of Rec. sci.* 1 (4), 41–42.
- Aizebeokhai, A.P., Oyeyemi, K.D., Joel, E.S., 2016. Groundwater potential assessment in a sedimentary terrain, southwestern Nigeria. *Arabian Journal of Geosciences* 9 (7), 496.
- Anudu, Goodluck K., Stephenson, Randell A., Macdonald, David I.M., 2014. Using high-resolution aeromagnetic data to recognise and map intra-sedimentary volcanic rocks and geological structures across the Cretaceous middle Benue Trough, Nigeria. *J. Afr. Earth Sci.* 99, 625–636.
- Barbara, N., Antonella, B., Brunella, R., Raffaele, B., 2016. Analysis of complex regional databases and their support in the identification of background/baseline compositional facies in groundwater investigation: developments and application examples. *J. Geochem. Explor.* 164, 3–17.
- Biswas, A., Jana, A., Sharma, S.P., 2012. Delineation of groundwater potential zones using satellite remote sensing and geographic information system techniques. A case study from Ganjam district, Orissa, India. *Research Journal of Recent sci* 1 (9), 59–66.
- Descloitres, M., Chalikakis, K., Legchenko, A., Moussa, A.M., Oï, M., 2013. Investigation of groundwater resources in the KomaduguYobe valley (lake Chad basin, Niger) using MRS and TDEM methods. *J. Afr. Earth Sci.* 87, 71–85.
- EPA, 1993. Use of Airborne, Surface, and Borehole Geophysical Techniques at Contaminated Sites. Office of Research and Development, Washington DC, 20460, pp. 3–1 – 3-9.
- Goussev, S.A., Charters, R.A., Peirce, J.W., Glenn, W.E., 2003. The meter reader Jackpine magnetic anomaly: identification of a buried meteorite impact structure. *Lead. Edge* 22, 740–741.
- Joel, E.S., Olasehinde, P.I., De, D.K., Omeje, M., Adewoyin, O.O., 2016. Estimation of aquifer transmissivity from geo-physical data. A case study of covenant university and environs, southwestern Nigeria. *Science International - Lahore* 28 (4), 3379–3385.
- Jones, H.A., Hockey, R.D., 1964. The geology of part of southwestern Nigerian. *Bulletin of the Geological Surv.of Nigeria* 31, 101.
- Keller, G.V., Frischknecht, F.C., 1966. *Electrical Methods in Geophysical Prospecting*. Pergamon Press, New York, p. 517.
- MacLeod, I., Vieira, S., Chaves, A.C., 1993. Analytic Signal and Reduction-To-The-Pole in the Interpretation of Total Magnetic Field Data at Low Magnetic Latitudes. *Third International Congress of the Brazilian Geophysical Society, Rio de Janeiro*, pp. 830–835.
- McLachlan, P.J., Chambers, J.E., Uhlemann, Binley, S.S., 2017. A. Geophysical characterisation of the groundwater-surface water interface. *Adv. Water Resour.* 109, 302–319.
- Miller, H.G., Singh, V., 1994. Potential field tilt – a new concept for the location of potential field sources. *J. Appl. Geophys.* 32, 213–217.
- Nabighian, M.N., 1972. The analytic signal of two-dimensional magnetic bodies with polygonal cross-section - its properties and use for automated anomaly interpretation. *Geophysics* 37, 507–517.
- Offodile, M.E., 2002. *Groundwater Study and Development in Nigeria*, second ed. Mecon Geology and Engineering services Limited, Jos, pp. 259–276. Published by.
- Ojo, J.S., Olorunfemi, M.O., Bayode, S., Akintorinwa, O.J., Omosuyi, G.O., Akinluyi, F. O., 2015. GIS integrated geomorphological, geological and geoelectrical assessment of the groundwater potential of akure metropolis, southwest Nigeria. *J. Earth Sci. Geotech. Eng.* 51 (4), 85–101.
- Olasehinde, P.I., 2010. *The Groundwater of Nigeria: A Solution to Sustainable National Water Needs*. Inaugural Lecture Series 17. Federal University of Technology, Minna Niger State.
- Omole, D.O., 2013. Sustainable groundwater exploitation in Nigeria. *J. Water Resour. Ocean Sci.* 2 (2), 9–14.
- Omole, D.O., Ndambuki, J.M., 2014. Sustainable living in africa: case of water, sanitation, air pollution & energy. *Sustainability* 6 (8), 5187–5202.
- Oyeyemi, K.D., Aizebeokhai, A.P., Ndambuki, J.M., Sanuade, O.A., Olofinnade, O.M., AdagunodoT, A., Oloajo, A.A., Adeyemi, G.A., 2018. Estimation of aquifer hydraulic parameters from surficial geophysical methods: a case study of Ota, Southwestern Nigeria. *IOP Conf. Ser. Earth Environ. Sci.* 173, 012028. <https://doi.org/10.1088/1755-1315/173/1/012028>.
- Prieto, C., Morton, G., 2003. New insights from a 3D earth model. *deepwater Gulf of Mexico: Lead. Edge* 22, 356–360.
- Reyment, R.A., 1965. *Aspects of the Geology of Nigeria*. University Press, Ibadan, Nigeria, pp. 23–73.
- Roest, W.R., Verhoef, J., Pilkington, M., 1992. Magnetic interpretation using the 3-D analytic signal. *Geophysics* 57, 116–125.
- Salem, A., Williams, S., Fairhead, J.D., Ravat, D., Smith, R., 2007. Tilt depth method: a simple depth estimation method using first-order magnetic derivatives. *Lead. Edge* 26, 1502–1505. <https://doi.org/10.1190/1.2821934>.
- Telford, W.M., Geldart, L.P., Sheriff, R.E., 1990. *Applied Geophysics*. University Press, New York, pp. 62–522. Cambridge.
- Thurston, J.B., Smith, R.S., 1997. Automatic conversion of magnetic data to depth, dip, and susceptibility contrast using the SPI (TM) method. *Geophysics* 62, 807–813. <https://doi.org/10.1190/1.1444190>.
- Verduzco, B., Fairhead, J.D., Green, C.M., MacKenzie, C., 2004. New insights into magnetic derivatives for structural mapping. *Lead. Edge* 23, 116–119.
- Vouillamoz, J.M., Lawson, F.M.A., Yalo, N., Descloitres, M., 2015. Groundwater in hard rocks of Benin: regional storage and buffer capacity in the face of change. *J. Hydrol.* 520, 379–386.
- Wijns, C., Perez, C., Kowalczyk, P., 2005. Theta map: edge detection in magnetic data. *Geophysics* 70, L39–L43.

## Update

# Groundwater for Sustainable Development

Volume 13, Issue , May 2021, Page

DOI: <https://doi.org/10.1016/j.gsd.2021.100593>





## Erratum regarding missing Declaration of Competing Interest statements in previously published articles

Declaration of Competing Interest statements were not included in the published version of the following articles that appeared in previous issues of <<Groundwater for Sustainable Development>>

The appropriate Declaration/Competing Interest statements, provided by the Authors, are included below.

1. "Parameterisation of physical models to configure subsurface characteristics of groundwater basins" [Groundwater for Sustainable Development, 2019; 9C: 100255] 10.1016/j.gsd.2019.100255

Declaration of competing interest: The Authors have no interests to declare.

2. "Height Above Nearest Drainage (HAND) model coupled with lineament mapping for delineating groundwater potential areas (GPA)" [Groundwater for Sustainable Development, 2019; 9C: 100256] 10.1016/j.gsd.2019.100256

Declaration of competing interest: The Authors have no interests to declare.

3. "An experimental approach to estimate groundwater temperature from 18O fractionation" [Groundwater for Sustainable Development, 2019; 9C: 100257] 10.1016/j.gsd.2019.100257

Declaration of competing interest: The Authors have no interests to declare.

4. "Improvement of glass solar still performance using locally available materials in the southern region of Algeria" [Groundwater for Sustainable Development, 2019; 9C: 100258] 10.1016/j.gsd.2019.100258

Declaration of competing interest: The Authors have no interests to declare.

5. "Modeling potential groundwater recharge in the Limpopo River Basin with SWAT-MODFLOW" [Groundwater for Sustainable Development, 2019; 9C: 100260] 10.1016/j.gsd.2019.100260

Declaration of competing interest: The Authors have no interests to declare.

6. "Applying the System of Environmental and Economic Accounts for Water (SEEA-Water) for integrated assessment of water security in an aquifer scale - Case study: Azarshahr aquifer, Iran"

[Groundwater for Sustainable Development, 2019; 9C: 100261] 10.1016/j.gsd.2019.100261

Declaration of competing interest: The Authors have no interests to declare.

7. "Evaluation of groundwater suitability for domestic and agricultural utility in semi-arid region of Anantapur, Andhra Pradesh State, South India" [Groundwater for Sustainable Development, 2019; 9C: 100262] 10.1016/j.gsd.2019.100262

Declaration of competing interest: The Authors have no interests to declare.

8. "Factors controlling arsenic contamination and potential remediation measures in soil-plant systems" [Groundwater for Sustainable Development, 2019; 9C: 100263] 10.1016/j.gsd.2019.100263

Declaration of competing interest: The Authors have no interests to declare.

9. "Integration of aeromagnetic and electrical resistivity imaging for groundwater potential assessments of coastal plain sands area of Ado-Odo/Ota in southwest Nigeria" [Groundwater for Sustainable Development, 2019; 9C: 100264] 10.1016/j.gsd.2019.100264

Declaration of competing interest: The Authors have no interests to declare.

10. "Conceptual hydrogeological and numerical groundwater flow modelling around the moab khutsong deep gold mine, South Africa." [Groundwater for Sustainable Development, 2019; 9C: 100266] 10.1016/j.gsd.2019.100266

Declaration of competing interest: The Authors have no interests to declare.

11. "Rainwater harvesting: Practiced potential for Integrated Water Resource Management in drought-prone Barind Tract, Bangladesh" [Groundwater for Sustainable Development, 2019; 9C: 100267] 10.1016/j.gsd.2019.100267

Declaration of competing interest: The Authors have no interests to declare.

12. "Various techniques to enhance distillate output of tubular solar still: A review" [Groundwater for Sustainable Development, 2019; 9C: 100268] 10.1016/j.gsd.2019.100268

DOIs of original article: <https://doi.org/10.1016/j.gsd.2019.100268>, <https://doi.org/10.1016/j.gsd.2019.100270>, <https://doi.org/10.1016/j.gsd.2019.100267>, <https://doi.org/10.1016/j.gsd.2019.100262>, <https://doi.org/10.1016/j.gsd.2019.100263>, <https://doi.org/10.1016/j.gsd.2019.100264>, <https://doi.org/10.1016/j.gsd.2019.100266>, <https://doi.org/10.1016/j.gsd.2019.100255>, <https://doi.org/10.1016/j.gsd.2019.100258>, <https://doi.org/10.1016/j.gsd.2019.100271>, <https://doi.org/10.1016/j.gsd.2019.100260>, <https://doi.org/10.1016/j.gsd.2019.100261>, <https://doi.org/10.1016/j.gsd.2019.100256>, <https://doi.org/10.1016/j.gsd.2019.100257>, <https://doi.org/10.1016/j.gsd.2019.100273>.

<https://doi.org/10.1016/j.gsd.2021.100593>

Available online 19 April 2021

2352-801X/© 2021 Published by Elsevier B.V.

Declaration of competing interest: The Authors have no interests to declare.

13. "Spatial assessment of groundwater vulnerability using DRASTIC model with GIS in uppar odai sub-watershed, Nandiyar, Cauvery Basin, Tamil Nadu" [Groundwater for Sustainable Development, 2019; 9C: 100270] 10.1016/j.gsd.2019.100270

Declaration of competing interest: The Authors have no interests to declare.

14. "Sensitivity analysis of groundwater vulnerability using DRASTIC method: A case study of National Capital Territory, Delhi, India"

[Groundwater for Sustainable Development, 2019; 9C: 100271] 10.1016/j.gsd.2019.100271

Declaration of competing interest: The Authors have no interests to declare.

15. "Groundwater conditions related to climate change in the semi-arid area of western Iran" [Groundwater for Sustainable Development, 2019; 9C: 100273] 10.1016/j.gsd.2019.100273

Declaration of competing interest: The Authors have no interests to declare.